Proc. Natl. Acad. Sci. USA
Vol. 86, pp. 5136–5140, July 1989
Medical Sciences

Molecular dissection of a contiguous gene syndrome: Frequent submicroscopic deletions, evolutionarily conserved sequences, and a hypomethylated "island" in the Miller–Dieker chromosome region

(lissencephaly/mental retardation/human chromosome 17/mouse chromosome 11/variable number of tandem repeats)

DAVID H. LEDBETTER*†, SUSAN A. LEDBETTER*, PETER VANTUINEN*, KIM M. SUMMERS*, TERENCE J. ROBINSON*, YUSUKE NAKAMURA‡, ROGER WOLFF‡, RAY WHITE‡, DAVID F. BARKER§, MARGARET R. WALLACE¶, FRANCIS S. COLLINS¶, AND WILLIAM B. DOBYNS||

*Institute for Molecular Genetics, Baylor College of Medicine, Houston, TX 77030; ‡Howard Hughes Medical Institute and §Department of Medical Informatics, University of Utah School of Medicine, Salt Lake City, UT 84132; ¶Howard Hughes Medical Institute and Departments of Internal Medicine and Human Genetics, University of Michigan, Ann Arbor, MI 48109; ||Department of Neurology, Medical College of Wisconsin, Milwaukee, WI 53201

Communicated by Victor A. McKusick, April 7, 1989

ABSTRACT **The Miller–Dieker syndrome (MDS), composed of characteristic facial abnormalities and a severe neuronal migration disorder affecting the cerebral cortex, is caused by visible or submicroscopic deletions of chromosome band 17p13. Twelve anonymous DNA markers were tested against a panel of somatic cell hybrids containing 17p deletions from seven MDS patients. All patients, including three with normal karyotypes, are deleted for a variable set of 5–12 markers. Two highly polymorphic VNTR (variable number of tandem repeats) probes, YNZ22 and YNH37, are codeleted in all patients tested and make molecular diagnosis for this disorder feasible. By pulsed-field gel electrophoresis, YNZ22 and YNH37 were shown to be within 30 kilobases (kb) of each other. Cosmid clones containing both VNTR sequences were identified, and restriction mapping showed them to be <15 kb apart. Three overlapping cosmids spanning >100 kb were completely deleted in all patients, providing a minimum estimate of the size of the MDS critical region. A hypomethylated island and evolutionarily conserved sequences were identified within this 100-kb region, indications of the presence of one or more expressed sequences potentially involved in the pathophysiology of this disorder. The conserved sequences were mapped to mouse chromosome 11 by using mouse–rat somatic cell hybrids, extending the remarkable homology between human chromosome 17 and mouse chromosome 11 by 30 centimorgans, into the 17p telomere region.**

Miller–Dieker syndrome (MDS) is a rare disorder manifested by characteristic facial abnormalities and classical, or type I, lissencephaly (smooth brain) (1). The facial abnormalities include bitemporal hollowing, prominent forehead, short nose with upturned nares, prominent upper lip, and micrognathia. The brain defect results from an arrest of neuronal migration at 10–14 weeks of embryonic development and affects the cerebral cortex with lesser involvement of the cerebellum and rhombic lip derivatives (2).

Based on reports of occasional familial recurrence, MDS was once thought to be an autosomal recessive disorder. It is now known that most cases of MDS have a subtle cytogenetic microdeletion of chromosome sub-band 17p13.3 that may be a *de novo* event or result from malsegregation of a familial balanced translocation (3, 4). Because high-resolution cytogenetic studies have failed to detect a visible deletion in some patients, other causal mechanisms must be considered such as a submicroscopic deletion in 17p or a single gene mutation in 17p or elsewhere. Preliminary studies have shown that some MDS patients have submicroscopic deletions that can be detected by several anonymous DNA markers within 17p13 (5, 6).

The high frequency of deletion and the lack of clear evidence for autosomal recessively inherited cases suggest that the MDS phenotype is due to deletion of more than one genetic locus. The highly consistent nature of the phenotype among these patients indicates that the number of critical loci may be relatively small, perhaps only two. Thus, MDS represents a model system for investigation of a "contiguous gene syndrome" (7)—i.e., a complex disease phenotype associated with chromosomal microdeletions affecting multiple, unrelated genetic loci physically contiguous on a chromosome. This well-defined chromosomal region on 17p is amenable to use of reverse genetics cloning strategies to identify expressed sequences that play a role in the pathophysiology of this disorder.

METHODS

Clinical and Cytogenetic Evaluation. The clinical diagnostic criteria used in previous studies (1, 5) have been modified slightly to include (*i*) severe type I lissencephaly with grossly normal or only mildly dysplastic cerebellum and (*ii*) characteristic facial abnormalities consisting of bitemporal hollowing, prominent forehead, short nose with upturned nares, prominent upper lip, thin vermillion border, and small jaw. Other facial changes, postnatal growth deficiency, and microcephaly are often but not always observed. When present, a midline calcification above or anterior to the third ventricle is probably pathognomonic. High-resolution chromosome analysis at approximately the 850-band stage (8) was performed on lymphocytes of all patients prior to construction of somatic cell hybrids.

Somatic Cell Hybrid Construction and Characterization. Standard polyethylene glycol fusions were performed between MDS patient fibroblast or lymphoblastoid cell lines and a mouse thymidine kinase-deficient (TK^-) cell line (9). Hybrid clones were selected in hypoxanthine/aminopterin/thymidine (HAT) medium to retain the segment of human chromosome 17 bearing the thymidine kinase gene at q23–q24. Cytogenetic analysis of somatic cell hybrids was performed by standard trypsin G-banding and sequential staining by the G-11 method to distinguish human from rodent chromosomal material. For MDS patients with normal karyo-

The publication costs of this article were defrayed in part by page charge payment. This article must therefore be hereby marked "*advertisement*" in accordance with 18 U.S.C. §1734 solely to indicate this fact.

Abbreviations: MDS, Miller–Dieker syndrome; RFLP, restriction fragment length polymorphism; VNTR, variable number of tandem repeats; HTF, *Hpa* II tiny fragment.

†To whom reprint requests should be addressed.

types, hybrids retaining a single chromosome 17 were identified cytogenetically. Clones containing the maternal or paternal chromosome 17 were distinguished by restriction fragment length polymorphism (RFLP) analysis using polymorphic markers outside the MDS region.

For mapping in mouse, two mouse–rat somatic cell hybrids were used. F(11)J is a microcell hybrid containing mouse chromosome 11 as its only mouse chromosome (10). RTM9 contains an 11;13 Robertsonian fusion as its only mouse chromosome (11).

Conventional Southern Blot Analysis. DNA from whole blood, lymphoblastoid cells, and somatic cell hybrids was isolated by routine methods and digested with restriction endonucleases (4 units/μg of DNA) as recommended by the supplier (Boehringer Mannheim). Agarose gel electrophoresis, capillary DNA transfer, hybridization, and washing were done as described (9).

Pulsed-Field Gel Electrophoresis. High molecular weight DNA in agarose plugs (12, 13) was digested with 20–40 units of enzyme according to the supplier's recommendations. *Saccharomyces cerevisiae* chromosomes and bacteriophage λ DNA concatemers were used as high molecular weight size markers. A *Bam*HI/*Eco*RI digest of adenovirus 2 DNA (IBI), with 13 fragments ranging in length from 35.9 to 1.7 kilobases (kb), provided lower-range molecular weight markers.

The LKB Pulsaphor system was used following the manufacturer's recommendations for voltage and pulse times. The gels were run in 60 mM Tris/60 mM boric acid/1 mM EDTA, pH 8.3, for 20–40 hr. A pulse time of 100 sec was used to resolve fragments in the 40- to 1000-kb range, 25 sec to resolve 40–400 kb, and 5 sec to resolve 20–100 kb. The gels were treated with 0.25 M HCl for 10 min followed by denaturation in 0.4 M NaOH for 40 min. Capillary transfer to GeneScreen*Plus* (DuPont) in 1.5 M NaCl/0.15 M sodium citrate, pH 7, was carried out for 16–20 hr.

Probes. pYNZ22 (*D17S5*), pYNH37 (*D17S28*), and p144-D6 (*D17S34*) are highly polymorphic VNTR (variable number of tandem repeats; ref. 14) probes that have been mapped to 17p13.3 (5). Probes EW501 (*D17S65*), EW502 (*D17S66*), EW504 (*D17S68*), EW506 (*D17S126*), EW507 (*D17S127*), VAW508 (*D17S128*), and VAW509 (*D17S129*) (hereafter referred to by their 500 series numbers) are polymorphic anonymous sequences isolated from chromosome 17-specific libraries and mapped distal to p11.2 (ref. 15; D.F.B., unpublished data). Cosmid P13 was isolated by screening a library constructed from a human–mouse hybrid containing human chromosome 17 as its only human chromosome (Y.N., unpublished data). Probe L53 contains a 5-kb insert in a λ Charon-3A derivative that was isolated from a *Not* I linking library constructed directly from flow-sorted chromosome 17 material (16).

Plasmid and phage DNA were isolated by standard methods and labeled with [α-^{32}P]dCTP by the random primer method. Hybridizations were carried out in 1 M NaCl/1% SDS/10% dextran sulfate containing denatured salmon sperm DNA (200 μg/ml) at 65°C for 12–16 hr. Before hybridization of whole cosmid or phage clones, both the probe and the filters were prehybridized with human placental DNA (500 μg/ml) to block repetitive sequences (17).

RESULTS

Clinical and Cytogenetic Characterization. Clinical diagnosis of MDS was confirmed in all patients by the criteria summarized above. Clinical descriptions and cytogenetics results of patients MDS-1 and -2 (3), MDS-A and -5 (4), MDS-6 (ref. 1; also reported as patient H.D. in ref 6), and MDS-9 (5) have been reported. Patient MDS-12 was the first child of unrelated parents. Pregnancy was complicated by polyhydramnios, but she did not require resuscitation after delivery. Her weight and length at birth were normal. An omphalocele was surgically closed during the first week of life. Facial appearance and neurologic problems were typical of MDS. She died at age 3 years from pneumonia. A cranial computerized tomography scan and examination of the brain at autopsy showed severe type I lissencephaly with no midline calcification and with mild cerebellar dysplasia. Cytogenetic analysis showed a small terminal deletion of 17p [46,XX,del(17) (p13.3)].

MDS Deletion Mapping Panel. MDS deletion chromosomes in somatic cell hybrids are illustrated in Fig. 1. Of the seven hybrids, four are from MDS patients with visible deletions and three are from patients with normal karyotypes. Hybrids JW4, FW1, MH74, and BR8 have been described (5). Hybrid JW4 (MDS-5) contains the largest MDS deletion observed to date (breakpoint estimated at 17p13.105), hybrid MH74 (MDS-1) contains the smallest visible deletion previously described (breakpoint in 17p13.3), and hybrid FW1 (MDS-A) contains a deletion of intermediate size (breakpoint estimated at 17p13.108). Hybrid BR8 contains the paternal chromosome 17 from an MDS patient with normal karyotype in which a *de novo* paternal deletion of YNZ22 and YNH37 was previously demonstrated (5).

New hybrids include AYI (MDS-12), containing a chromosome 17 with a visible deletion (breakpoint in 17p13.3), and two hybrids from MDS patients with normal karyotypes

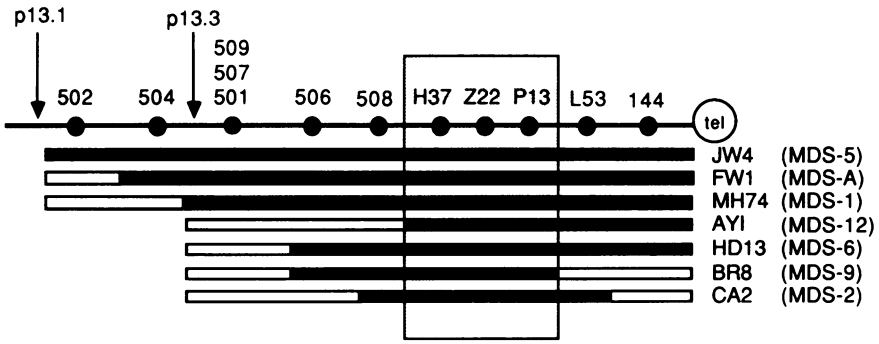

FIG. 1. Twelve anonymous probes are ordered within band p13 based on their presence or absence in hybrids containing deletion chromosomes 17 from seven MDS patients. Probes are ordered from centromere (left) to telomere (tel). Visible breakpoints at sub-bands p13.1 and p13.3 are designated by arrows. Below the map are bars representing the results of hybridization of the 12 probes, with hybrid name (and patient designation) to the right. Filled bars represent negative hybridization (deletion), and open bars represent positive hybridization (not deleted). The top four hybrids (JW4, FW1, MH74, and AYI) are from patients with cytogenetically visible deletions, and the results are consistent with these being terminal deletions. The bottom three hybrids (HD13, BR8, and CA2) are from patients with normal karyotypes, two of which (BR8 and CA2) proved to have interstitial deletions. The smallest region of overlap among all seven deletions is indicated by the box and includes probes YNH37 and YNZ22 and cosmid P13.

(MDS-2 and MDS-6). For the latter patients, the two chromosome 17 homologs were distinguished by RFLP analysis as described (5). For both patients, YNZ22 and YNH37 are deleted in hybrids containing one homolog but not in hybrids containing the other. These two hybrids (CA2 and HD13) were included in the mapping panel for characterization of new anonymous probes.

Localization of 12 Probes Within 17p13. YNZ22, YNH37, and 144-D6 had previously been mapped to 17p13. A total of 9 additional anonymous probes failed to recognize DNA from the hybrid with the largest MDS deletion (hybrid JW4) and therefore map to 17p13. These 12 probes were hybridized to DNA from the MDS deletion hybrids and the results are shown in Fig. 1. Probe 502 is the most proximal, being deleted in hybrid JW4 (MDS-5) but not in hybrid FW1 (MDS-A). This distinguishes these two breakpoints on a molecular level and confirms the cytogenetic interpretation that MDS-5 has a more proximal breakpoint. Probe 504 is deleted in JW4 (MDS-5) and FW1 (MDS-A) but not in MH74 (MDS-1); therefore, it is distal to 502.

Patient MDS-1 has a well-characterized cytogenetic breakpoint that clearly lies within band 17p13.3 (3). The size of this deletion, involving a single prometaphase sub-band at the 850-band stage of resolution (8), is estimated at <3000 kb. Ten of the 12 probes are deleted in hybrid MH74 (MDS-1), localizing them to the most distal sub-band, 17p13.3.

Probes YNH37, YNZ22, and P13 are deleted in all seven patients, including the three with normal karyotypes, suggesting that all three probes are within the MDS critical region. Five probes (501, 506, 507, 508, and 509) are deleted in MH74 (MDS-1) but not in AYI (MDS-12). This indicates that MDS-12 has a smaller visible deletion than MDS-1 and that these five probes are proximal to the critical region. Probe 508 is deleted in all three karyotypically normal patients and is the closest marker to the critical region on the centromere side. Probe 506 is deleted in two of the three karyotypically normal patients and is proximal to 508.

The *Not* I linking clone L53 maps distal to YNZ22 by virtue of its deletion in AYI (MDS-12) but presence in BR8 (MDS-9). This is consistent with the previous finding that patient MDS-9 has an interstitial rather than terminal deletion (5), and sets the distal boundary of the MDS critical region between YNZ22 and L53. The third VNTR probe, 144D6, is deleted in all patients with visible deletions and was previously shown by linkage analysis to be distal to YNH37 and YNZ22 (18). This probe is not deleted in hybrids from two of the karyotypically normal patients, BR8 (MDS-9) and CA2 (MDS-2), consistent with both having interstitial deletions. Since 144D6 is deleted in hybrid HD13 (MDS-6) from the third karyotypically normal patient, we cannot presently determine whether her deletion is interstitial or terminal. Alternatively, this patient may represent a cryptic unbalanced translocation, whose molecular analysis would be indistinguishable from that of a terminal deletion.

Pulsed-Field Analysis of the MDS Critical Region and Identification of a Hypomethylated Island. Somatic cell hybrid mapping served to order the 12 probes into eight intervals along 17p13 but did not provide any information regarding the distance between probes, nor did it allow us to estimate the size of the critical region now localized between probes 508 and L53.

To determine the distance between the two VNTR probes within the critical region (YNZ22 and YNH37), pulsed-field gel electrophoresis was performed on lymphoblastoid cells from normal individuals. YNH37 detected two *Sal* I fragments of 700 and 350 kb in two unrelated individuals (Fig. 2 *Left*), presumably representing partial methylation of one *Sal* I site. A small *Sfi* I fragment was observed whose size was difficult to estimate on this gel. When the filter was stripped and hybridized to YNZ22, the same *Sal* I and *Sfi* I fragments were detected (Fig. 2 *Right*). To more accurately determine the size of the shared *Sfi* I fragment, conditions were altered to resolve smaller fragments.

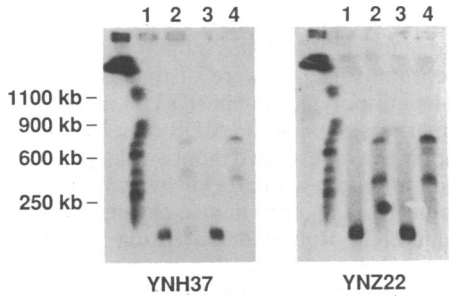

FIG. 2. Pulsed-field gel electrophoresis with probes YNH37 (*Left*) and YNZ22 (*Right*). DNA samples from lymphoblastoid cells (6×10^6 cells per ml) from two normal individuals (lanes 1 and 2 and lanes 3 and 4) were digested with *Sfi* I (lanes 1 and 3) or *Sal* I (lanes 2 and 4). A 100-sec pulse time was used and the gel was run for 20 hr. *S. cerevisiae* chromosomes are in the far left lane and sizes in kilobases are given. After hybridization to YNH37, the filter was stripped and hybridized to YNZ22, and identical fragment sizes were observed for both *Sfi* I and *Sal* I.

With the use of a pulse time of 5 sec for 20 hr to resolve fragments in the 20- to 100-kb range, YNH37 detected an *Sfi* I fragment of ≈29 kb (Fig. 3 *Left*). The *Bss*HII digest also showed a fragment of ≈29 kb, and the *Not* I digest showed a 60-kb fragment. The filter was stripped and hybridized to YNZ22 (Fig. 3 *Right*). YNZ22 detected a 29-kb *Sfi* I fragment identical to that observed with YNH37, indicating that the two VNTR probes are very close to each other. Extremely small fragments (4.7 and 3.4 kb) were observed with *Not* I and *Bss*HII. This significant clustering of unmethylated CpG sites is indicative of an HTF (*Hpa* II tiny fragment) island (19) around YNZ22.

Cosmid P13 detected the same 350- and 700-kb *Sal* I fragments as YNZ22 and YNH37 but detected different fragments for *Sfi* I (42 and 100 kb), *Not* I (340 kb), and *Bss*HII (150 kb). The flanking probes 508 and L53 did not share any

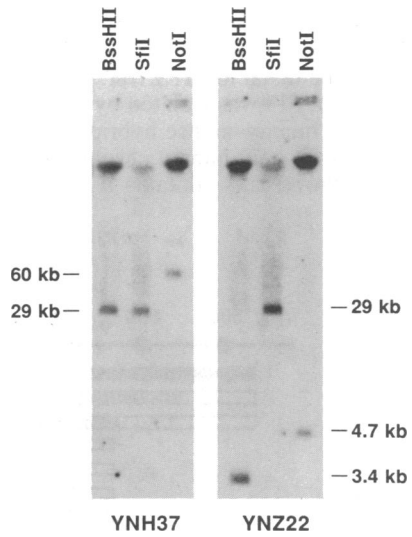

FIG. 3. Pulsed-field gel electrophoresis with 5-sec pulse time for 20 hr to resolve fragments in the 20- to 100-kb range. Results shown are from lymphoblastoid cells of one normal individual but are representative of similar experiments with several unrelated normal controls. For YNH37 (*Left*), *Bss*HII and *Sfi* I digests showed fragments of ≈29 kb, while the *Not* I digest showed a 60-kb fragment. The filter was stripped and hybridized to YNZ22 (*Right*), which detected the same 29-kb *Sfi* I fragment as YNH37. Very small fragments (<5 kb) were detected for both *Bss*HII and *Not* I.

fragments in common with YNZ22, YNH37, or P13 with six different enzymes (*Bss*HII, *Not* I, *Sfi* I, *Nru* I, *Mlu* I, and *Sal* I). Thus, using complete digestions with these enzymes, we were unable to determine the distance between 508 and L53.

Cosmid Clones Containing Both YNH37 and YNZ22. The close proximity of YNZ22 and YNH37 was confirmed by analysis of 14 independently derived YNZ22 cosmid clones. Hybridization of YNH37 to these cosmid clones showed that 4 of 14 were positive for YNH37 sequences. Restriction mapping of several overlapping cosmids confirmed that YNH37 and YNZ22 shared an *Sfi* I fragment of ≈25 kb (size varied depending on the allele sizes of YNH37 and YNZ22 of individual clones) and indicated that the two sequences are actually within 15 kb of each other (Fig. 4). The very small *Bss*HII and *Not* I fragments detected by YNZ22 on pulsed-field analysis were also confirmed. There were four *Not* I sites, four *Bss*HII sites, and four *Sfi* I sites within a 7-kb region around YNZ22, confirming the presence of an HTF island.

Two overlapping YNZ22 cosmids, c81-2 and 13A, were shown by restriction mapping to extend at least 25 kb proximal (c81-2) and 30 kb distal (13A) to the 15-kb fragment containing YNZ22 and YNH37. The independently isolated cosmid P13 was found by hybridization and restriction mapping to partially overlap with 13A and extended an additional 30 kb in the telomere direction. These three overlapping cosmids cover a total of >100 kb of genomic DNA, and all three are completely deleted in the seven MDS deletion hybrids. This provides a minimum estimate of 100 kb for the smallest region of overlap among these seven deletions.

Evolutionarily Conserved Sequences That Map to Mouse Chromosome 11. Plasmid YNH37 was previously noted (P.v.T. and D.H.L., unpublished data) to cross-hybridize to mouse genomic DNA on Southern blots at moderate to high stringency. Plasmid YNZ22 did not cross-hybridize to rodent sequences. However, hybridization of cosmid clones containing YNZ22 but not YNH37 showed several fragments that did cross-hybridize to mouse DNA. In both cases, subcloning has shown that the cross-hybridizing sequences are unique and do not contain the VNTR repeats themselves. Cosmid P13 also contains multiple fragments that cross-hybridize to mouse and hamster. This evolutionary conservation is further indirect evidence of one or more expressed sequences within this 100 kb of the MDS critical region.

Cross-hybridization to mouse enabled us to map these probes to a specific mouse chromosome. Human chromosome 17 has extensive homology with mouse chromosome 11, in that every locus on human chromosome 17 that has been mapped in mouse is on chromosome 11 (20). Plasmid YNH37 (Fig. 5) and cosmid clone 13A hybridized to DNA from a mouse–rat hybrid containing mouse chromosome 11 as its only mouse chromosome, confirming the prediction that these probes are on mouse chromosome 11. A second mouse–rat hybrid containing a mouse Robertsonian 11;13 translocation as its only mouse material was also positive (data not shown). YNH37 and YNZ22 are ≈30 centimorgans

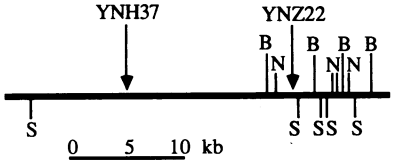

FIG. 4. Restriction map of cosmid c81-2, containing both YNH37 and YNZ22 VNTR sequences. Single and double digests were performed with *Sfi* I (S), *Bss*HII (B), *Not* I (N), and *Eco*RI (not shown). YNH37 and YNZ22 were found to be within 15 kb of each other, and YNZ22 is surrounded by an HTF island comprising four *Sfi* I sites, four *Bss*HII sites, and four *Not* I sites within a 7-kb region.

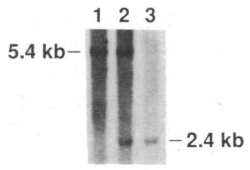

FIG. 5. Localization of YNH37 to mouse chromosome 11. Southern blot of *Hin*dIII-digested DNA was probed with YNH37. Lane 1, control rat DNA; lane 2, DNA from a mouse–rat hybrid cell line containing mouse chromosome 11 as its only mouse DNA; lane 3, control mouse DNA. The characteristic 2.4-kb mouse band is present in the mouse–rat hybrid and therefore localizes YNH37 to mouse chromosome 11. A characteristic rat band is seen at 5.4 kb.

distal to the myosin heavy chain (*MYH2*) locus on human chromosome 17 (18). Since *MYH2* was previously the most distal 17p locus mapped to mouse chromosome 11, our results significantly extend the linkage homology between these two chromosomes (Fig. 6).

DISCUSSION

To begin the molecular dissection of the MDS chromosome region, we have localized 12 anonymous DNA markers to 17p13, 10 of which are in the most distal sub-band p13.3. Four MDS patients with visible cytogenetic deletions are deleted for 5–12 of these probes, while three patients with normal karyotypes are deleted for a variable set of 5–7 markers. No evidence of "hotspots" for chromosome breakage in the MDS region was obtained, as seven patients showed six different breakpoints on the proximal side of the critical region, and the two proven interstitial deletion patients showed different breakpoints on the distal side (Fig. 1). Despite this heterogeneity in breakpoints, all seven patients are deleted for three probes—YNZ22, YNH37, and P13—within a smallest region of overlap of at least 100 kb.

The high frequency of large molecular deletions is consistent with the hypothesis that deletion of more than one locus must occur to produce the MDS phenotype. A requirement for deletion is further supported by RFLP and densitometry data for eight additional MDS patients (total 15/15 patients) who are deleted for YNZ22 and YNH37 (ref. 5; D.H.L., unpublished data). It therefore appears that all or at least the

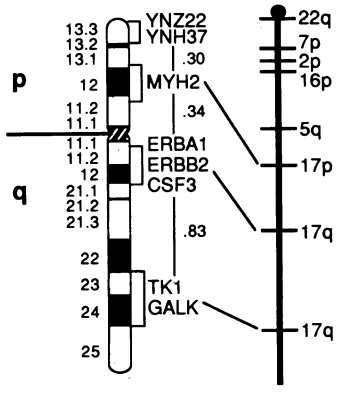

FIG. 6. Comparison of human chromosome 17 (*Left*) and mouse chromosome 11 (*Right*). Physical locations (9) of selected genes on human 17 are indicated by brackets, and genetic distances between loci are given as total recombination distance estimated from the complete linkage map of Nakamura *et al.* (18). Human genes include thymidine kinase (*TK1*) and galactokinase (*GALK*) at q23–24; *ERBA1*, *ERBB2*, and granulocyte colony-stimulating factor (*CSF3*) at q11.2–12; and myosin heavy chain (*MYH2*) at 17p12. Their approximate positions on the genetic map of mouse chromosome 11 (20) are indicated. The proximal portion of mouse chromosome 11 comprises loci from human chromosomes 22q, 7p, 2p, 16p, and 5q.

great majority of MDS patients will have cytogenetically detectable or large molecular deletions. This significantly decreases the possibility of an autosomal recessive form of MDS and indicates that a combination of cytogenetic and molecular diagnostic studies should be performed on all such patients. Since YNZ22 and YNH37 are highly polymorphic, deletion analysis by RFLP studies is possible for most patients. Many of the close flanking markers (e.g., 506, 508, and 144D6) are also polymorphic and are useful for deletion analysis.

The present data provide indirect evidence that there is one or more expressed sequence within this 100 kb of the MDS critical region. YNZ22 is within a large HTF island; such an island is frequently associated with the 5′ region of eukaryotic genes (19). YNZ22 and P13 cosmid clones, as well as plasmid YNH37, detected evolutionarily conserved sequences in mouse, hamster, and rat, a degree of conservation suggestive of exon sequences. We have so far been unable to detect a unique transcript in mRNA from human or mouse tissues, due to extensive cross-hybridization of these G+C-rich probes to 28S ribosomal RNA. That two VNTR probes identified evolutionarily conserved sequences and an HTF island in this region may not be completely fortuitous. Several VNTR or minisatellite sequences have been identified in introns or flanking regions of genes, although no function or consistent structural relationship has been identified. These include the insulin gene (21), *HRAS* oncogene (22), type II collagen gene (23), and five minisatellite sequences in the vicinity of the α-globin gene cluster at the 16p telomere (24).

The evolutionary conservation of both probes allowed us to map them to mouse chromosome 11. Every locus on human chromosome 17 that has been mapped in mouse is on mouse chromosome 11 (20), a degree of linkage conservation unusual for autosomal loci. Our results extend this remarkable homology by an additional 30 centimorgans on the human map, to the terminal portion of human 17p. Knowledge of the chromosomal location in mouse and the extensive homology between human chromosome 17 and mouse chromosome 11 may facilitate a search for a mouse model for MDS, as at least seven neurological mutants are known on mouse chromosome 11 (25, 26).

Although these two VNTR probes were independently isolated from cosmid libraries (14), pulsed-field analysis and identification of cosmid clones containing both sequences showed that they are within 15 kb of each other. The third VNTR probe, 144-D6, is located telomeric to YNZ22 and YNH37, although its distance is not known. The finding of three VNTR sequences in close proximity in the 17p telomere is of interest in light of the recent observations that human minisatellite sequences are preferentially localized in telomeric regions and that multiple, unrelated minisatellite sequences may be closely linked to each other (27). In addition, it has been suggested that minisatellite sequences may be hotspots for recombination (28), a possibility indirectly supported by the correlation of their telomeric clustering and the increased recombination frequency observed in telomeric regions, especially in males (18, 27). This increased recombination is evident in 17p, in which 15% recombination in males was observed between YNZ22 and 144D6 (18), a frequency 5 times higher than that in females and extremely high for a physical distance estimated at <3000 kb. The possibility therefore exists that unequal recombination events associated with VNTR sequences clustered in 17p13 may be involved in the mechanism for producing *de novo* interstitial deletions or interchromosomal translocations. This would predict a paternal bias in the origin of *de novo* deletions in MDS, consistent with preliminary observations (5, 6).

We thank Cynthia Curry, M.D., for patient referral, Dr. Ann Killary for hybrid F(11)J, Dr. David R. Cox for hybrid RTM9, and Donna R. Rich, M.S., for technical assistance. This work was supported by National Institutes of Health Grant HD20619 (D.H.L.). F.S.C. and M.R.W. acknowledge support from the Howard Hughes Medical Institute and National Institutes of Health Grant GM34960. D.F.B. acknowledges support from the National Neurofibromatosis Foundation and National Institutes of Health Grant CA28854.

1. Dobyns, W. B., Stratton, R. F. & Greenberg, F. (1984) *Am. J. Med. Genet.* **18,** 509–526.
2. Dobyns, W. B. (1987) *Birth Defects Orig. Artic. Ser.* **23,** 225–241.
3. Dobyns, W. B., Stratton, R. F., Greenberg, F., Nussbaum, R. L. & Ledbetter, D. H. (1983) *J. Pediatr.* **102,** 552–558.
4. Stratton, R. F., Dobyns, W. B., Airhart, S. D. & Ledbetter, D. H. (1984) *Hum. Genet.* **67,** 193–200.
5. vanTuinen, P., Dobyns, W. B., Rich, D. C., Summers, K. M., Robinson, T. J., Nakamura, Y. & Ledbetter, D. H. (1988) *Am. J. Hum. Genet.* **43,** 587–596.
6. Schwartz, C. E., Johnson, J. P., Holycross, B., Mandeville, T. M., Sears, T. S., Graul, E. A., Carey, J. C., Schroer, R. J., Phelan, M. C., Szollar, J., Flannery, D. B. & Stevenson, R. E. (1988) *Am. J. Hum. Genet.* **43,** 597–604.
7. Schmickel, R. D. (1986) *J. Pediatr.* **109,** 231–241.
8. ISCN (1985) in *International System for Human Cytogenetic Nomenclature,* eds. Harnden, D. G. & Klinger, H. P. (Karger, Basel).
9. vanTuinen, P., Rich, D. C., Summers, K. M. & Ledbetter, D. H. (1987) *Genomics* **1,** 374–381.
10. Killary, A. M. & Fournier, R. E. (1984) *Cell* **38,** 523–534.
11. Joyner, A. L., Lebo, R. V., Kan, Y. W., Tjian, R., Cox, D. R. & Martin, G. R. (1985) *Nature (London)* **314,** 173–175.
12. Schwartz, D. C. & Cantor, C. R. (1984) *Cell* **67,** 67–75.
13. van Ommen, G. J. B. & Verkerk, J. M. H. (1986) in *Human Genetic Diseases: A Practical Approach,* ed. Davies, K. E. (IRL, Oxford), pp. 113–133.
14. Nakamura, Y., Leppert, M., O'Connell, P., Wolff, R., Holm, T., Culver, M., Martin, C., Fujimoto, E., Hoff, M., Kumlin, E. & White, R. (1987) *Science* **235,** 1616–1622.
15. Fain, P. R., Barker, D. F., Goldgar, D. E., Wright, E., Nguyen, K., Carey, J., Johnson, J., Kivlin, J., Willard, H., Mathew, C., Ponder, B. & Skolnick, M. (1987) *Genomics* **1,** 340–345.
16. Wallace, M. R., Fountain, J. W., Brereton, A. M. & Collins, F. S. (1989) *Nucleic Acids Res.* **17,** 1665–1677.
17. Litt, M. & White, R. L. (1985) *Proc. Natl. Acad. Sci. USA* **82,** 6206–6210.
18. Nakamura, Y., Lathrop, M., O'Connell, P., Leppert, M., Barker, D., Wright, E., Skolnick, M., Kondoleon, S., Litt, M., Lalouel, J.-M. & White R. (1988) *Genomics* **2,** 302–309.
19. Bird, A. P. (1987) *Trends Genet.* **3,** 342–347.
20. Buchberg, A. M., Brownell, E., Nagata, S., Jenkins, N. A. & Copeland, N. G. (1989) *Genetics* **122,** 153–161.
21. Bell, G. I., Selby, M. J. & Rutter, W. J. (1982) *Nature (London)* **295,** 31–35.
22. Capon, D. J., Chen, E. Y., Levinson, A. D., Seeburg, P. H. & Goeddel, D. V. (1983) *Nature (London)* **302,** 33–37.
23. Stoker, N. G., Cheah, K. S. E., Griffin, J. R., Pope, F. M. & Solomon, E. (1985) *Nucleic Acids Res.* **13,** 4613–4622.
24. Jarman, A. P. & Higgs, D. (1988) *Am J. Hum. Genet.* **43,** 249–256.
25. Green, M. C. (1981) in *Genetic Variants and Strains of the Laboratory Mouse* (Fisher, Stuttgart, F.R.G.), pp. 8–278.
26. Lane, P. W., Ganser, A. L., Kerner, A.-L. & White, W. F. (1987) *J. Hered.* **78,** 353–356.
27. Royle, N. J., Clarkson, R. E., Wong, Z. & Jeffreys, A. J. (1988) *Genomics* **3,** 352–360.
28. Jeffreys, A. J., Wilson, V. & Thein, S. L. (1985) *Nature (London)* **314,** 67–73.